Chapter 1
General Introduction

The motivation for the present investigation on the development of electrocatalysts for Hydrogen Evolution Reaction (HER) is described in this chapter. A brief discussion on the reasons why these electrocatalysts do not reach the full potency to replace fossil fuels in the hydrogen economy and the strategies that need to be embraced to develop an efficient catalyst are also discussed.

Chapter 1

1.1 Current energy resources and related issues:

In the past few decades, the rapid increase in population along with lifestyle advances has put a huge demand on the amount of energy consumption. Till now 82% of the world's energy is extracted from fossil fuels (**Figure 1.1**) [1]. But its limited availability and unsustainable nature is a major threat to the fossil fuel sources. Also, fossil fuel usage has a severe effect on the environment causing sustained and increased carbon emissions, leading to global warming. According to International Energy Agency (IEA) report CO_2 emission from energy combustion alone grew up to 423 Mt in 2022. If CO_2 emission continues to rise at this rate the earth will have to face bitter environmental change including extended droughts, damaging storms, rising sea levels, annihilation of the vital ecosystem elements, etc. This is a major concern and impacts every inhabitant of this planet [2]. Therefore, focus of scientific research, in tune with the advances in civilization in recent years, has shifted to developing clean, sustainable, and renewable energy sources which can replace fossil fuels.
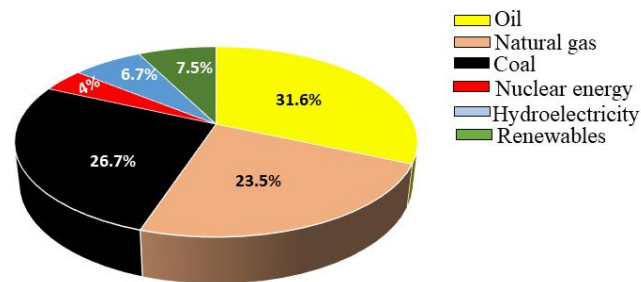

Figure 1.1 Energy resources for worldwide energy consumption according to the data of 2023 Statistical Review of World Energy.

Among all the possible renewable energy sources, solar energy is the most promising one [3]. As per a 2008 report, the global energy consumed in the year 2008 is almost equivalent to the energy of sunlight striking the earth for only 70 minutes [4]. It is presumed that only 1% of the land needs to be covered with photoelectrochemical cells of ~10 % equivalent efficiency to harvest sufficient energy for global needs by 2050 [5]. Nevertheless, solar energy is an intermittent

energy source due to which it is important to be stored. A number of methods have been invented to store this energy. The best possible methods are:

i) converting low energy water molecules into high energy hydrogen molecules *via* the water splitting reaction in the presence of sunlight as a means of storage of light energy in form of chemical bond energy, and

ii) solar energy is collected on a panel, and then stored using supercapacitor or battery in the form of electrochemical energy [6].

Hydrogen is a very unique molecule and energy carrier. Rising demand for finding a greener energy source is totally dependent on fuel cell technology that can be an environment friendly way of producing energy [7]. Research community has explored a number of energy carrier molecules in fuel cell like methanol, ethanol, propane, hydrogen, biodiesel, etc. for possible substitution of fossil fuels. Among all of them, hydrogen happens to be the best candidate to substitute fossil fuels because of its lightweight, highest possible energy density, and zero greenhouse gas emission property (**Figure 1.2**) [8]. And regarding energy density, hydrogen is about three times more energetic than gasoline [9].
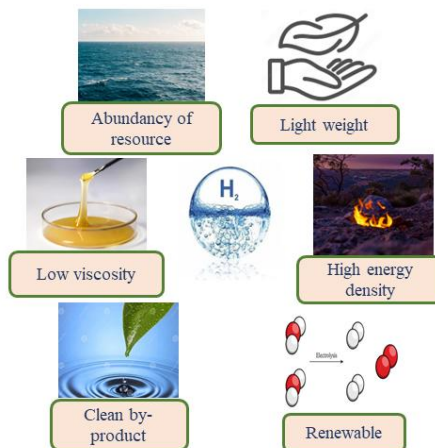

Figure 1.2 Advantages of hydrogen as a fuel obtained from water splitting.

The most common practices for hydrogen production are mentioned below.

1] Steam reforming, which is a very high-temperature method (700-1000^{0}C). Here, high-temperature steam is passed over hydrocarbon in the presence of a nickel catalyst to generate hydrogen and carbon monoxide. Produced carbon monoxide is

further reacted with steam for a greater yield of hydrogen. In this process, carbon dioxide is generated as by product [10].

 2] Thermochemical water splitting produces hydrogen as a result of a series of chemical reactions. These reactions proceed at very high temperatures (500-2000^{0}C) [11].

3] Photo-biological system, where green microalgae and cyanobacteria use light energy to split water or a variety of bio-based mass to generate hydrogen [12].

4] In the gasification method, high temperature (>700^{0}C) is used to generate hydrogen from coal or biomass [10].

5] Electrolysis utilizes external voltage to split water into hydrogen at the cathode (+) and oxygen at the anode (-).

6] In the photoelectrochemical method, semiconducting materials are used to produce hydrogen from water splitting using only light energy [10].

Ironically, vast majority of commercial hydrogen production is dependent upon fossil fuels (**Figure 1.3**), which is opposite to our intention as steam reforming of natural gas releases greenhouse gases (CO_2, CO, etc.) in tremendous amounts into the atmosphere.
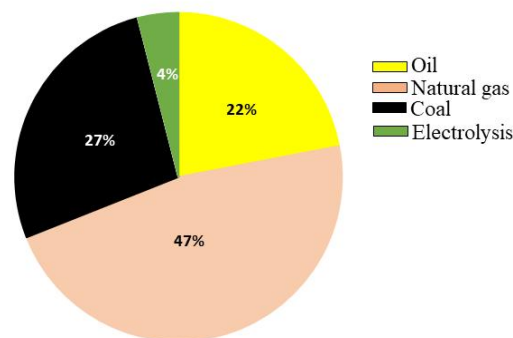

Figure 1.3 Different sources used for hydrogen production according to International Renewable Energy Agency (IRENA) 2021.

Among the other mentioned approaches, electrolysis, and photoelectrolysis are the two most favourable environmentally friendly methods for hydrogen production, wherein water splits into hydrogen and oxygen with the aid of a catalyst. It draws
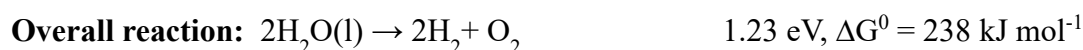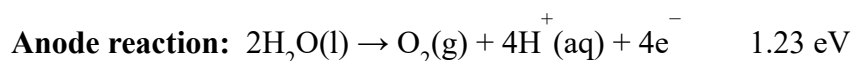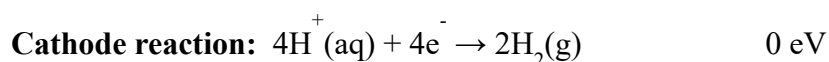
immense attention as during this process 1) high purity hydrogen is produced, 2) clean and useful by-product (oxygen) is produced [13] and 3) no high-temperature, high-pressure reactors are required. Also, the abundance of the resource makes the process sustainable [14].

1.2 Hydrogen evolution *via* water splitting reaction:

Nature converts solar energy to chemical energy and store it. The process is called photosynthesis. During this process, light energy is used to extract electrons from water to generate a strong reducing species, nicotinamide adenine dinucleotide phosphate hydrogen (NADPH), which donates its electrons to generate carbohydrate molecules from atmospheric CO_2 [15]. The essence of the process lies in the storage of light energy in the form of chemical bonds. The modern approach of producing hydrogen is to mimic natural photosynthesis where solar energy is stored in the high energy, dense chemical bonds of hydrogen [16]. Water splitting reactions can be carried out in alkaline, neutral or acidic medium. The efficiency of the reaction in alkaline conditions is low as the hydrogen evolution reaction (HER) kinetics in these conditions solely depend on the passive anodic oxygen evolution reaction (OER) kinetics. Whereas in the acidic medium, already existing protons make HER more efficient [17]. Hence the urge to carry out HER in acidic conditions is greater. An efficient water splitting reaction will be the one where the following redox reaction proceeds significantly [18].

HER in acidic medium:

Cathode reaction: $4H^+(aq) + 4e^- \rightarrow 2H_2(g)$ 0 eV

Anode reaction: $2H_2O(l) \rightarrow O_2(g) + 4H^+(aq) + 4e^-$ 1.23 eV

Overall reaction: $2H_2O(l) \rightarrow 2H_2 + O_2$ 1.23 eV, $\Delta G^0 = 238$ kJ mol^{-1}

To capture the oxidized and reduced products, a membrane that is compatible with the redox reactions is inserted [19]. It also facilitates the passage of electrons and protons. HER can be driven photochemically, electrochemically or photoelectrochemically.

Chapter 1

1.2.1 Photochemical water splitting

The photocatalytic approach requires a semiconductor that provides an electron-hole pair upon excitation, a sacrificial electron donor that can effectively quench the photosensitizer, and a proton reduction catalyst that transforms solar energy into chemical energy [20] (**Figure 1.4**). This is an endothermic process as low energy water molecules convert to the high energy hydrogen molecules. Therefore, an external energy supply is required to carry out the reaction. In photocatalytic HER, photon energy acts as the external energy supplier. Theoretical calculation shows that water splitting requires 1.23 eV which is equivalent to energy of wavelength of 1009 nm. Although a large proportion of photons possesses this much energy, since water is transparent to ultraviolet (UV)-visible light, in actuality photons with a wavelength shorter than 190 nm can accomplish this reaction [4]. This is why even though the photocatalytic approach seems to be more convenient for direct conversion of sunlight energy, the efficiency of this method remains quite low for commercial approval.
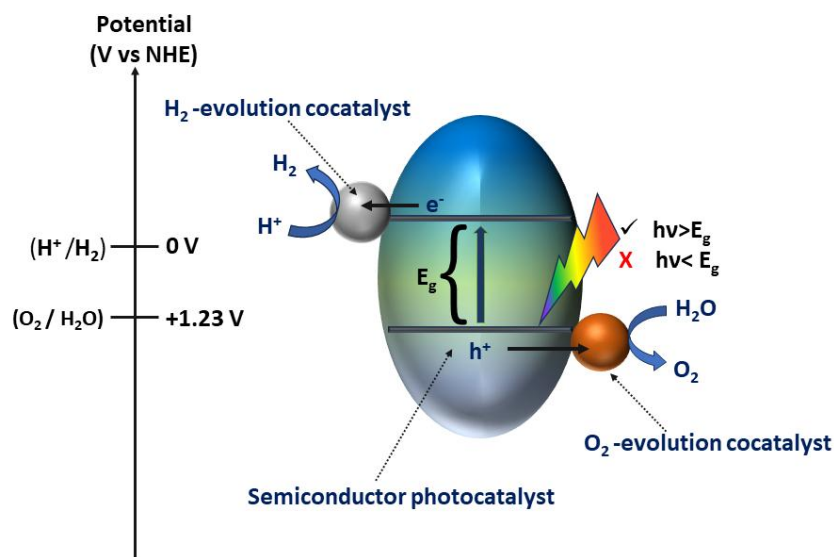

Figure 1.4 Schematic representation of the photocatalytic water splitting reaction.

Chapter 1

1.2.2 Photoelectrochemical water splitting

For a more efficient approach, photoelectrochemical water splitting seems to be more favourable than photolysis of water [21]. The concept of photoelectrochemical cell was first presented by Fujishima and Honda (**Figure 1.5**). During the process, a pack of photons gets absorbed on the semiconductor surface. Upon exceeding the photon energy than that of the semiconductor band gap, an electron hole-pair generates. The electron is then conducted to the cathode by an external circuit leaving behind a hole on the photoanode surface. Thus, in the cathode hydrogen is generated whereas photogenerated holes are exhausted by an oxidation reaction [22,23].
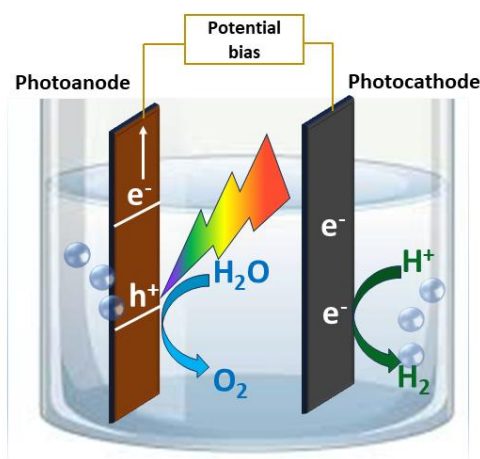

Figure 1.5 Schematic representation of photoelectrocatalytic water splitting reaction.

It is noteworthy that to drive the oxygen evolution half-reaction, the photo-induced holes should have a potential more positive than 1.23 V and the photo-excited electrons should have a potential more negative than 0 with respect to the normal hydrogen electrode (NHE) scale [24,25]. Therefore, to carry out photoelectrolysis, the choice of the semiconductor is quite important regarding its valence band (VB) and conduction band (CB) positions in terms of energy. In the following diagram, we have presented a comparison of the band gap of photoelectrocatalysts and their alignment with respect to the redox reactions involved with the water-splitting reaction (**Figure 1.6**) [26].
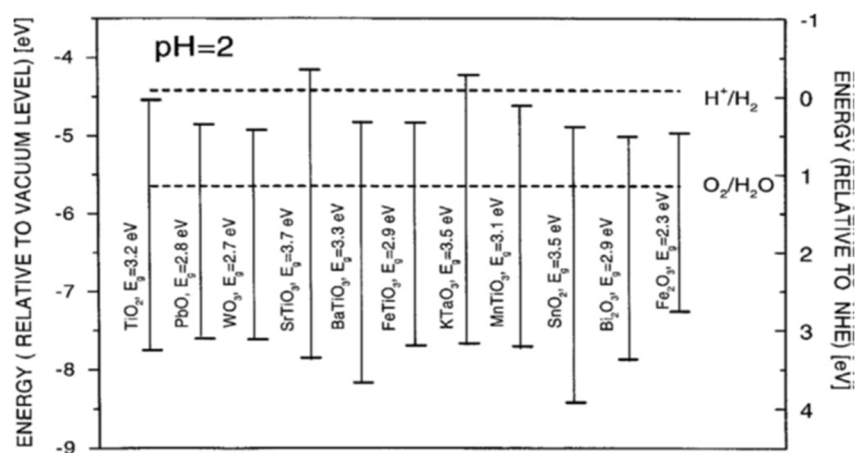
Figure 1.6 Band energy states of various semiconductors [26].

1.2.3 Electrochemical water splitting

Unlike photocatalysis/ photoelectrolysis, in electrocatalysis electrons are delivered from the anode to the cathode with the help of an external potentiostat which is sufficient enough to carry out HER at a reasonable catalytic overpotential [27]. In **Figure 1.7** the classic three-electrode compartment used in the lab for electrocatalytic HER is presented. Here the synthesized catalyst is drop-casted on a glassy carbon electrode (GCE) that serves as a working electrode (anode), Pt wire/ graphite electrode as the cathode, and silver/silver chloride (Ag/AgCl) is used as the reference electrode.
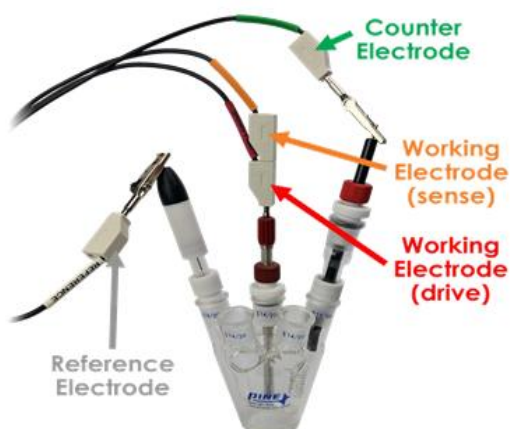

Figure 1.7 Three-electrode cell compartment used in the laboratory to study electrocatalytic HER.

In electrocatalytic HER, sunlight energy is not used directly. However, the sustainability of this method can be increased by conjugating the external energy supplier to solar panels or to supercapacitors where solar energy is stored. Even though this electrolysis approach requires a solid-liquid interface that introduces a reaction microenvironment that may differ from the bulk solution [28], it is significantly less complex and also more efficient than photocatalysis. This method has been acclaimed as a potential candidate to recuperate the problems of environmental crisis as a result of the combustion of fossil fuels and is considered to be more efficient than both photocatalytic and photoelectrocatalytic water splitting.

1.3 Mechanism involved in hydrogen evolution reaction:

As we mentioned above, water splitting reaction *via* the electrolysis process is a combination of two half-cell reactions: 1) hydrogen evolution reaction at the cathode and 2) oxygen evolution reaction at the anode. But between these two reactions, the one that generates hydrogen under ambient conditions draws the major attention as it has the potential to become a sustainable energy source. Water electrolysis is mainly carried out in neutral, alkaline and acidic mediums. Protons are the precursors of HER and in acidic medium plenty of protons are available making hydrogen evolution more facile as the reaction kinetics does not have to solely depend on the sluggish kinetics of OER. In an acidic medium, HER proceeds *via* two possible mechanisms of multistep reactions: 1) the Volmer Heyrovsky mechanism and 2) the Volmer Tafel mechanism (**Figure 1.8**) [29]. The final mechanism is a combination of two of the three steps.

1. Discharging protons on active sites of the electrode surface to generate adsorbed hydrogen (H_{ads}), which is known as the Volmer step. This step is common in both mechanisms.

2. Subsequently, there are two different pathways to generate hydrogen molecules. The mechanism proceeds in either of the pathways depending on the active site coverage H_{ads} [30].

i] In case of low surface coverage of H_{ads}, the adsorbed H atoms will readily combine with a proton (as protons are more mobile) and an electron to produce an H_2 molecule. This is the Volmer-Heyrovsky mechanism.

$$H_{ads} + H^+ (aq) + e^- \rightarrow H_2 (g).$$
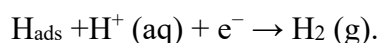
ii] If surface H_{ads} coverage is high, two adjacent H_{ads} will interact with each other resulting in the formation of an H_2 molecule which is the Volmer-Tafel mechanism.

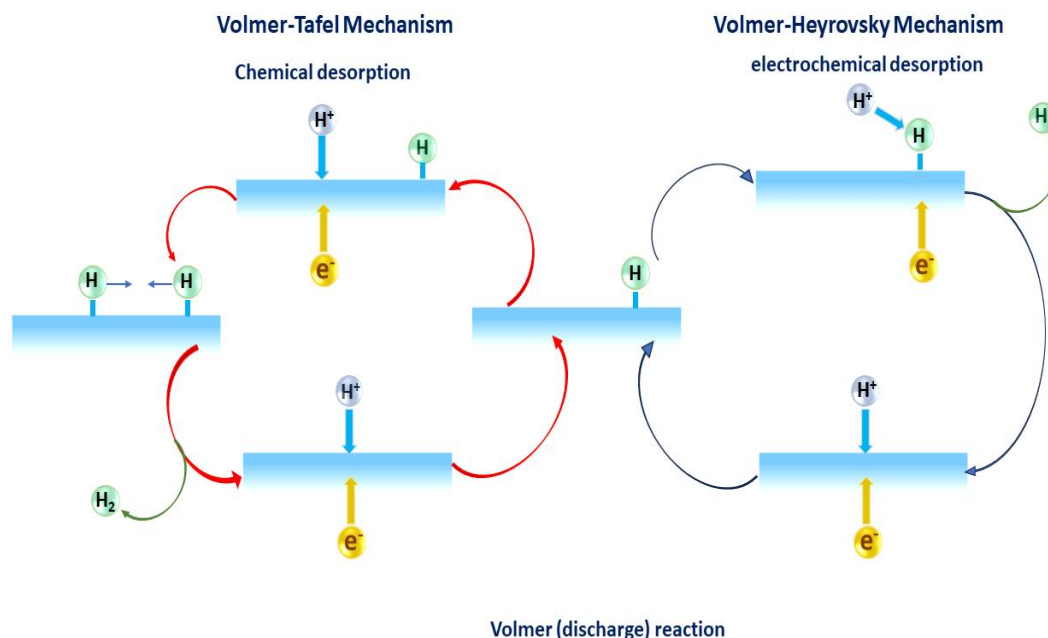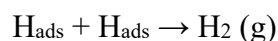$$H_{ads} + H_{ads} \rightarrow H_2 \text{ (g)}$$

Figure 1.8 HER mechanisms and various steps involved in each of them.

The efficiency of HER kinetics mainly depends on the strength of the M-H bond (M= active metal site). In the case of weak M-H interaction, Volmer step becomes the rate-determining step (RDS). In metals where M-H interaction is quite strong, the adsorption of H^+ on the active site is fast, and hence either Tafel or Heyrovsky steps become the RDS. In 1913, a French chemist Paul Sabatier stated that the best catalyst would be the one that binds to the reactant in its intermediate state with a strength that is neither too weak nor too strong [31]. So, the best HER catalyst is where the catalyst-H_{ads} interaction is moderate, or in other words, where the free energy of H_{ads} (ΔG_{Hads}) = 0. The effectiveness of different catalysts towards HER is visualized using the Sabatier Volcano plot (**Figure 1.9**) where ΔG_{Hads} on the catalytic surface is plotted against either one of the parameters, exchange current density (i_0) or the current density at a specific overpotential or turn over frequency (TOF) value of HER [32]. It is termed as the Volcano plot because when ΔG_{Hads} is plotted against any one of the above parameters then it takes the shape of a volcano.
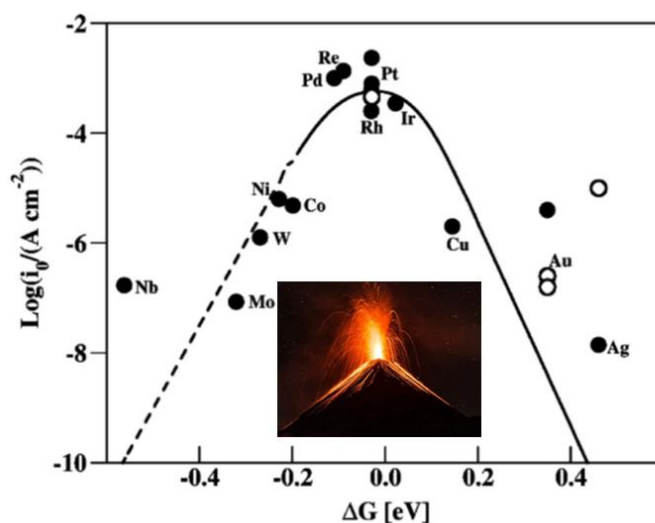
Figure 1.9 Relationship between i_0 and ΔG on HER volcano plot [33].

The volcano plot was first plotted for metals in 1972 by Trasatti and his research group [34]. The decrease in the current density after the optimal M-H bond strength can be interpreted as an over-stabilization of the absorbed intermediate. On the left part of the plot, there are catalysts where Tafel or Heyrovsky is the RDS and at the right side of the plot, those catalysts where ΔG_{Hads} is quite high and hydrogen becomes increasingly unstable, Volmer step is the RDS. Catalysts near the apex of the plot are considered the best catalysts for HER [35]. Ideally, Pt is positioned at the apex of the volcano plot making it the best active catalyst as all the reaction steps for HER on its surface are thermo-neutral. However, Pt is a scarce metal making the entire process quite irrelevant for practical application in terms of sustainability and cost effectiveness. An intensive study has been ongoing around the world to replace Pt with equally efficient yet cost-effective and earth-abundant materials.

1.3.1 Common HER catalysts

The closest entities of Pt in the Volcano plot are various transition metals. Incidentally, numerous studies also support that the best active and abundant HER electrocatalysts are mainly transition metal (Fe, Co, W, Ni, Mo, Cu)-sulphides [36-38], selenides [39], and phosphides [40].

i) Transition metal sulphides (TMSs): Commonly, TMSs are prepared using different methods including solvothermal [37], hydrothermal [41], microwave-

assisted method [42], metal evaporation technique via electron beam followed by thermal sulphidization [43], etc. The activity of several sulphide-based catalysts such as CoS, CoS_2, NiS_2, bimetallic Co-Fe-S, Co-Ni-S alloy have been explored towards HER [43-46]. The most studied metal sulphide in this aspect is MoS_2 [47]. However, initially, it was thought that MoS_2 was inactive towards HER. But interestingly the edge of MoS_2 possesses ΔG_{Hads} value close to 0.08 eV that actively participates in HER. Tard *et al.* presented a cost-effective route to synthesize FeS nanoparticles [37]. Although its efficiency is less remarkable than that of MoS_2 but the prolonged stability along with cheapness and abundance of the material established FeS as one of the promising HER catalysts.

ii) Transition metal selenides (TMSes): TMSes are prepared using different procedures that include solvothermal [48], hydrothermal [49] and thermal pyrolysis of metal oxide followed by selenization [50], and microwave irradiation techniques [51]. Studies reveal that TMSes are more conductive than the corresponding TMSs due to more electro-positivity of selenium ions. Metal selenides are known for their graphite-like layered structure which is held by Van der Waal's force and they have three main phases: 1T of octahedral coordination, and 2H and 3R of trigonal prismatic coordination [39]. But only 1T phase is metallic and enhances the overall catalyst activity. In layered structure, these active phases are not always exposed terminating the efficiency. Hence synthesising non-layered metal selenides is more desirable from the prerogative of charge transfer. Another concern is that similar to TMSs, the edge sites in TMSes are active but basal planes are predominating in the structure. So, another strategy could be to activate those inert basal planes. Wang *et al.* presented that when B atoms were doped in $MoSe_2$ structure, then the increased hybridization among B 2p, Mo 3d and Se 2p orbitals induced a number of states at the Fermi level resulting in reduction of the band gap and hence increase in the conductivity [52]. The overall increased charge transfer enhanced the HER activity to obtain the benchmark current density of 10 mAcm^{-2} at an overpotential of 84 mV. The catalytic activity of a number of selenides of Co, W and multi-metals have also been explored [39].

iii) Transition metal phosphides (TMPs): TMPs of only six transition metals (Fe, Co, Cu, Ni, Mo and W) are known to carry out HER [40]. Other synthesized TMPs of Ti, Zn, and Cd are immediately hydrolyzed in acidic or basic medium and hence

inactive for HER. Different approaches like solvothermal, electrodeposition, heating of the mixed metals and P source in an inert atmosphere, and chemical vapour deposition methods [53-56] are practiced to synthesize TMPs. P atoms can be seen as the dopant in the metal cluster. It offers a pivotal role in the activity of TMPs. Theoretical studies conducted by Wang *et al.,* Kibsgaard *et al.* and Tang *et al.* illuminated that ΔG_{Hads} value was negative (-0.34 eV) at relatively low H_{ads} coverage at the P edge site of the metal cluster, which was efficient enough to promote the adsorption of hydrogen and after full coverage of the surface with H_{ads}, the ΔG_{Hads} value most interestingly turned positive, which is responsible for fast hydrogen desorption making TMP an ideal candidate for HER [57-59]. Hence P atoms in the metal cluster are desirable for increased catalytic activity. Numerous metal phosphide with varying P content have been explored, e.g., Ni_2P, $Ni_{12}P_5$ and Ni_5P_4. Among these Ni_xP_{YS}, Ni_5P_4 contains the highest P content and exhibits the best catalytic activity as expected [60]. However, after reaching optimum P content, the electronegativity of the P atom causes delocalization of electrons resulting in poor electrical conductivity of the cluster [61]. Hence it is quite important to maintain the metal and P atomic ratio.

1.3.1.1 Role of heteroatoms (P, S, and Se) in transition metal phosphides, sulfides, and selenides

As mentioned above the P atom in TMPs attracts protons and thus discharge of protons becomes quicker and hence HER proceeds efficiently. A lot of related research reveals that more P content increases the HER kinetics. The negatively charged P atoms enhance the proton adsorption on the catalyst surface at low H_{ads} coverage whereas it acts reversibly at high H_{ads} coverage. A similar mechanism is followed by metal sulfides and selenides too. M-H_{ads} bond strength is the primary factor in determining desorption kinetics. Consequently, selenium is in the forefront than P and S due to the strength of the bonds S- H_{ads} (363 kJ mol^{-1}), P-H_{ads} (322 kJ mol^{-1}), and Se-H_{ads} (276 kJ mol^{-1}) [62]. Following this trend, sulfides of transition metals should be of lower activity in HER due to their high bond dissociation energy and higher electronegativity than P/Se. Even so, sulfides like CoS_2, CoS, MoS_2, and Ni_3S_2 are considered to be efficient HER catalysts.

Although these catalysts are quite active towards HER, it is not enough to prove them an efficient catalyst for commercialization. Several other factors need to be addressed for a material to be an effective HER catalyst.

1] The first one is that the synthesis method of the catalyst should be harmless to the user and mother nature.

2] The conductivity of the catalysts is another concerned factor. Although doping of metal or non-metal atoms (N, P, B, etc.) or ions is used to improve the conductivity, however, beyond a certain limit of the dopant concentration the activity falls apart and even sometimes makes the catalyst an insulated one.

3] Almost all the above-mentioned active catalysts exist in nano form. So, there is a high chance of agglomeration. Study reveals that in many catalysts, some particular edges or planes (e.g., MoS_2) are responsible for carrying out HER effectively rather than all the planes. In such a case, the agglomeration could possibly turn the active catalyst into an inactive one.

4] HER is more efficient in acidic conditions. To be efficient the catalyst should be operated for a long time in such an acidic environment. But many catalysts get corroded in such an environment making the entire process ineffective.

5] During efficient hydrogen evolution, the H_2 gas bubble formation increases on the active surface which detaches its contact with the reactive intermediate resulting in a decrease in the catalyst activity [63]. Hence, along with charge transfer, mass transfer should also be considered for an effective catalyst.

So, the scientific community has developed numerous strategies to develop efficient catalysts whilst trying to diminish these detrimental factors.

1.3.2 Various catalyst development strategies

1] Synthesizing metal oxide/hydroxide-based catalysts

It is of utmost importance for an active HER electrocatalyst to be synthesized by such a process that doesn't trigger any kind of pollution or hazardousness. Study reveals that apart from oxides and hydroxides of the transition metals, all other highly active HER catalysts are more or less harmful. In the past, metal oxide was not considered for HER due to its poor electrical conductivity, unsuitable ΔG_{Hads} value and limited catalytic active sites [64-66]. However, recent studies reveal that there are a number of ways to make them suitable for HER. The most common approaches

are creating oxygen vacancy sites, introducing surface strain, doing phase engineering, and doping metal or non-metal atoms or ions [67-72]. In 2016, Swaminathan *et al.* modified the TiO_2 structure by creating an oxygen vacancy site converting the stoichiometry of the titania structure to $TiO_{1.23}$ [73]. The filled excess electrons in the vacancy-induced site attracted the neighbouring Ti atoms by electronic interaction and thus facilitated charge transporting strikingly turning the site into metallic from nonconductive TiO_2. Another strategy is phase structure engineering. In 2019, Li *et al.* engineered Ti_2O_3 lattice in its three different unit cells (**Figure 1.10**) wherein the best HER activity was obtained in the case of cubic lattice. Their intensive research, along with theoretical findings suggested that HER efficiency increased with smaller charge transfer energy which was correlated with the stronger bond energy of Ti-O. Among all the experimented unit cells of Ti_2O_3, Li and his team claimed that the Ti-O hybridization was the strongest in γ-Ti_2O_3 which modulated the ΔG_{Hads} to the optimum level resulting in the best HER efficiency among two other unit cells [68]. Another approach includes metal/ non-metal doping and morphology engineering. Recently the activity of other oxide groups like spinel oxides, simple and double perovskites, and metal (oxy)hydroxides have also been explored towards HER [74,75,76,77].

γ- Ti_2O_3 (cubic)   o- Ti_2O_3 (orthorhombic) α- Ti_2O_3 (trigonal)
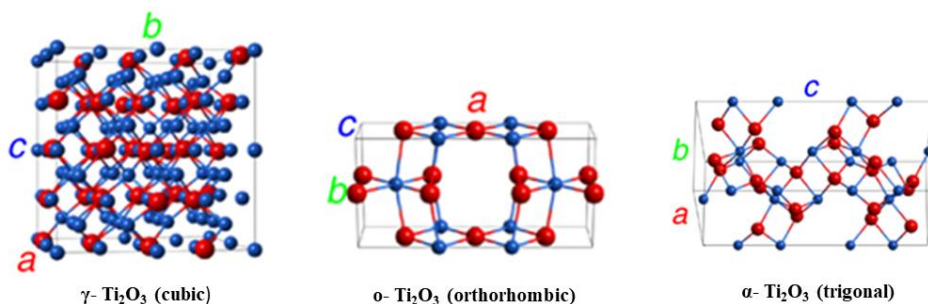
Figure 1.10 Different polymorphs of titanium oxide [68].

2] Modifying the morphology of the catalyst

i) In general, Nafion is used as a binder to coat the catalyst on the substrate. But sometimes even a little change in the proportion of added Nafion can provide extra resistance, inhibit the exposure of the active surface area and mass transfer of the catalyst [78,79]. To prevent this circumstance, synthesis of self-supported electrocatalyst is encouraged. The intimate active catalyst and surface contact also

enhance both charge and mass transfer. In 2018, Mishra *et al.* developed a CoP/Ni$_5$P$_4$/CoP sandwich-like structure **(Figure 1.11 (a))** where the substrate Ni$_5$P$_4$ was synthesized by *in situ* phosphorization of Ni foam [80]. The catalyst exhibited a long-term of stability up to 27 h without any noticeable degradation of current density. Abbott *et al.* developed *in situ* growth of Ni$_3$S$_2$ films on nanoporous carbon **(Figure 1.11 (b))** by a unique solvothermal method followed by a galvanic reaction [81]. The catalyst provided a robust durability of 111 h in an acidic environment without any loss of current density.
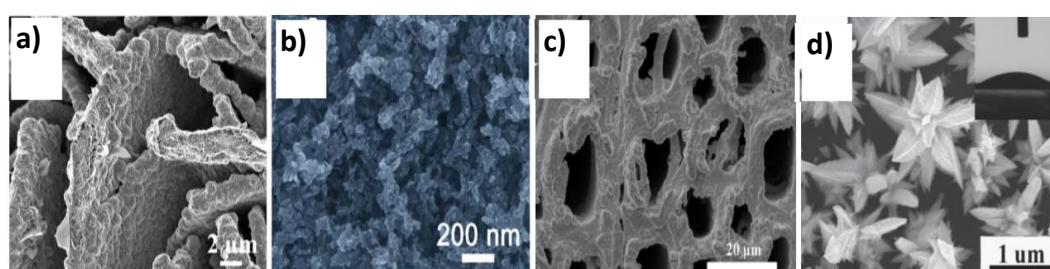

Figure 1.11 Various surface morphologies of the catalysts for HER to improve the reaction efficiency [80-83].

ii) H$_2$ bubble formed on the catalyst surface can block the reactive site hampering catalytic activity unless there is a proper channel for the mass transfer. Regarding this challenge, porous catalysts have been found to facilitate proper channels effective for bubble detachment. In 2020, Zhou *et al.* anchored NiP alloy in poplar wood to provide a number of fine channels which interestingly transported bubbles when they grew the same diameter as that of the channel without impeding the catalyst activity **(Figure 1.11 (c))** [82]. Due to this unique structure, the catalyst showed outstanding durability of 36 h under a large cathodic current density of 1200 mA cm^{-2}. Fabrication of super wettable catalyst is more favoured for bubble detachment. Different surface morphology including pine-shaped, needle-shaped, or even 3D frameworks is beneficial for the fabrication of super-aerophobic surface electrodes. A high bubble contact angle is favoured for enhanced mass transfer. Ziang *et al.* synthesized pine-shaped Pt nanostructured electrode that showed increased and steady hydrogen evolution **(Figure 1.11 (d))** [83]. The unique morphology played an important role in rapid bubble detachment due to the lower contact area of the bubble on the electrode surface and also the higher bubble contact angle than that of Pt

nanosphere and Pt flat surface. Liu *et al.* reported a cost-effective HC-MoS$_2$/Mo$_2$C catalyst that showed efficient mass transfer as a result of the reduced diameter of the formed H$_2$ bubbles than that of the Pt surface [84].

3] Increasing the intrinsic activity of the catalyst

i) By doping: The introduction of both metal (Fe, Co, Ni, Cu, etc.) and non-metal atoms (N, P, B, As) can modulate the electron density of the catalyst, and the optimum efficiency can be generated by tuning the dopant concentration. When the dopant atom is more electronegative than the parent atom, the electron-absorbing ability of the overall catalyst is enhanced. This increases the valence state of the host catalyst which, in turn, improves the intrinsic activity. Tsiakaras *et al.* synthesized N-doped Mo$_2$C that performed HER effectively [85]. N atom not only regulated the electronic structure of the carbon skeleton but also desirably distributed the Mo$_2$C active sites. Besides the aforementioned benefactions of the doping effect, synergistic cation and anion doping are more advantageous in the modulation of hydrogen adsorption energy. Doping of metal atoms enhanced the hydrogen adsorption on previously inert basal planes of MoS$_2$ but it didn't result in improvement of HER activity. Zheng *et al.* incorporated Se atoms into the Co-doped MoS$_2$ that enhanced the HER efficiency by balancing the strong M-H$_{ads}$ bonds [86].

ii) Alloying: The intrinsic activity of the catalyst can be increased by using bimetallic system which modulates the Fermi level via electron transfer mechanism to carry out HER efficiently [87,88]. Chen *et al.* pyrolyzed Ir-modified Fe-based metal-organic frameworks (MOFs) to synthesize IrFe nanoalloys supported on N-doped carbon layers [89]. Due to the electronegativity difference between Ir and Fe atoms the Fermi level of Ir got modulated and the electrons shifted near Ir atoms which resulted in the shifting of the d-band centre far away from the Fermi level. The resulting band structure led to the weakening of the catalyst surface-hydrogen interaction or in conclusion shifting the ΔG_{Hads} to 0.

iii) Modulating phase structure of the catalyst: Phase engineering can enhance the number of catalytic active sites and also the charge transfer and hence HER activity. For example, in comparison to non-layered transition metal dichalcogenides (TMDs), multilayered TMDs exhibit low performance for HER as electrons have to surmount the van der Waals forces between the layers to reach the outer active sites

since HER is a bulk phenomenon [90]. Moreover, in catalysts, all surfaces are not equally active for HER, e.g., even though Pt is considered to be the best HER catalyst all the sites are not equally active. For example, ΔG_{H*} values of (100) and (001) planes of α-MoB$_2$ are quite efficient towards HER at high H$_{ads}$ coverage that surpass the Pt (111) plane that cannot withstand the activity at high hydrogen coverage [91].

4] Using carbon support

Another widely used strategy is to use carbon materials as support for the metal catalysts which prevent the metal particles from agglomeration and promote the maximum exposure of the active site. The use of carbon material as a support for HER reaction has been studied since the initial days of the U.S. space program in the 1960s [92]. Because of its high abundance, corrosion resistivity, insolubility and outstanding electrical conductivity carbon has a wide range of energy-related applications that accounts for its extensive application in HER [93,94].
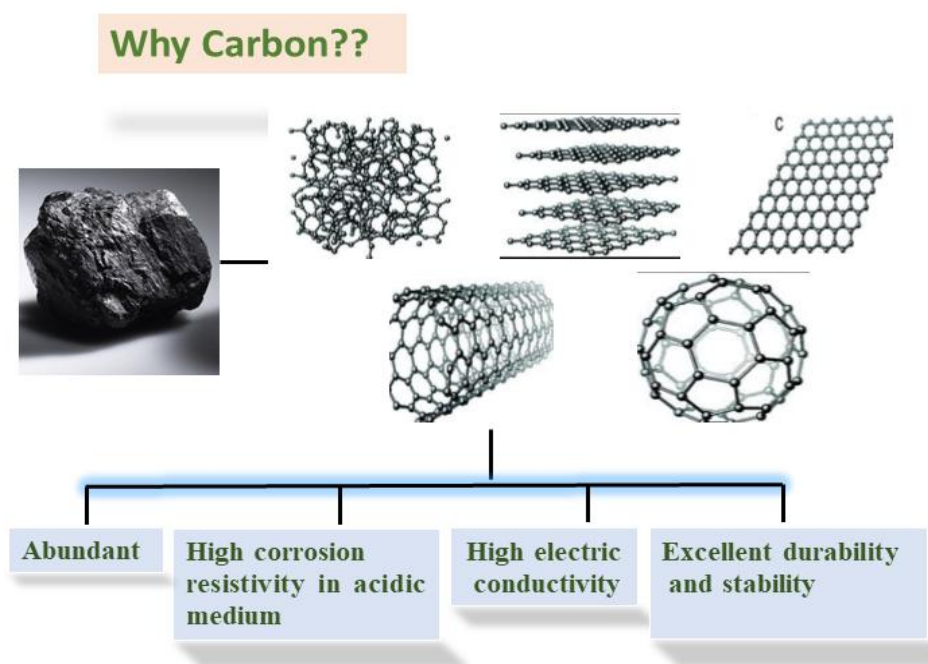

Figure 1.12 Different forms of carbon and its favorable properties for use in catalytic applications.

Different forms of carbon, e.g., 1D amorphous carbon, 2D graphene sheet, 3D single-walled or multi-walled carbon nanotube (SWCNT or MWCNT), reduced

graphene oxide (RGO) aerogel, fullerene, etc. have been explored as support materials **(Figure 1.12)** [95,96, 97,98,99,100]. Wang *et al.* embedded P-doped Mo_2N nanoparticles of average diameter of 4.4 nm in 3D vertically aligned carbon nanosheets which offered sufficient mechanical strength for nanoparticles and reduced the charge transport resistance [101] to carry out HER efficiently. Jiang *et al.* synthesized a porous structure of CoP derived from the Co MOF which was grown on RGO as a support. RGO rendered ultimate contact with the catalysts along with a conductive network which greatly enhanced the catalyst activity towards HER in both acidic and basic media [102]. The corrosion resistance property of the carbon materials enables its composites to withstand harsh acidic or alkaline conditions for long periods of time.

1.3.3 Electrical parameters to evaluate the catalytic activity

In electrocatalytic HER, it is important to measure a catalyst's efficiency that can be evaluated by several electrical parameters. Some of the basic parameters are discussed below:

1] Overpotential (η):

Theoretically, HER should take place at 0 eV. However, in practice each electrochemical reaction proceeds along with some kinetic barriers and shows far more deviation from the theoretically expected potential value based on the thermodynamic considerations. To overcome these hindrances, an extra electromotive force in terms of potential is required to move forward the electrochemical reactions which is called the overpotential and it is termed as 'η'. For HER, there are three prime sources of overpotential *viz.*, the activation overpotential, the concentration overpotential and the overpotential resulting from the resistance exercised by the electrochemical interfaces [103,104,105]. The activation overpotential is an inherent characteristic of the material that catalyses the HER. Hence, the only way to minimize this is by choosing an effective catalyst. Another one is the concentration overpotential that happens simultaneously with the electrode reaction due to the rapid concentration drop near the interfaces which can be reduced by stirring the electrolyte. The resistance overpotential is eliminated manually by subtracting the potential iR drop from the experimentally obtained potential value. In case of faster kinetics of the HER than the anodic OER, the

activation overpotential or the most common term onset overpotential is very important, the value of which is derived from the linear sweep voltammogram.

2] Tafel Slope

In an electrocatalytic process, Tafel plot is obtained by plotting the data obtained in polarization curves as log [current density(j)] *vs.* η. HER kinetics is predicted from the slope of the Tafel plot which is

$$b_{1,v} = 2.303\ RT\ /\ \alpha nF \qquad (1)$$

where b stands for the corresponding Tafel slope, R is the ideal gas constant, T is the temperature, F is the Faraday constant, α the symmetry factor of value 0.5 and n is the number of electrons transferred (n = 2 in the case of HER) [106,107].

It is determined that a catalyst with a high charge transfer ability should possess a low Tafel slope value due to which it is often considered as the basic parameter to predict the activity of the catalyst. In HER kinetics, the expected Tafel slope values are 118 mV dec^{-1}, 40 mV dec^{-1}, and ~30 mV dec^{-1} for Volmer, Heyrovsky, and Tafel reactions respectively. When the Tafel slope value comes at around 30 mV dec^{-1}, it is determined that the HER reaction proceeds *via* Volmer-Tafel mechanism. The Tafel slope value of ~120 mV dec^{-1} is said to follow the Volmer-Heyrovsky mechanism [103,104]. However, the Tafel slope obtained from the polarisation curve may lead us to misinterpret the catalytic activity as the current obtained is not a steady current. To remove this inaccuracy about the catalyst activity, a conventional practice can be utilized that entails the steady state current of the catalyst from the chronoamperometric curves obtained at a particular overpotential. Beyond the particular overpotential, the kinetics of HER is facile and almost all the catalysts follow the same HER kinetics. This simply indicates the direct correlation of exchange current density to the onset overpotential in HER. Thus, it has been adapted to evaluate the overpotential at a fixed current density (e.g., 10 mA cm^{-2}) and considered to be another prime parameter of the catalytic activity.

3] Stability

Another important parameter to establish a catalyst for successful commercial application is its stability. During the catalytic performance, bubbling due to hydrogen production sometimes tends to accumulate on the catalyst surface degrading the catalyst activity. Excessive bubbling due to intense hydrogen production can damage the material, therefore it is important to evaluate the catalyst regarding this parameter and test the catalyst stability over time. In many studies, the stability check has been carried out for more than ten-hour time periods [108]. Alternatively, cyclic voltammetry (CV) is also carried out for 1000 cycles and the change in overpotential is measured from a linear sweep voltammetry (LSV) curve before and after carrying out this CV measurement.

4] Mass and Specific Activities

Another two important active parameters to define the efficiency of an electrocatalyst are the mass and specific activities of the catalyst [109]. Mass activity is obtained by normalizing the current density of the electrocatalyst with the catalyst loading and is expressed in A g^{-1}. Specific activity is acquired by normalization of the current density by the electrochemical surface area (ECSA) or by the Brunauer-Emmett-Teller (BET) surface area and is expressed as A m^{-2} or mA cm^{-2}. The mass and specific activities of an electrocatalyst are more precise when considered at a specific overpotential.

The electrocatalytic activity of a material is best understood by evaluating the overpotential, Tafel slope, and stability parameters.

1.4 Supercapacitor

Apart from converting solar energy into chemical energy (*via* HER), another means to restore solar energy is the use of storage devices. Batteries and supercapacitors are two major energy storage devices [110].
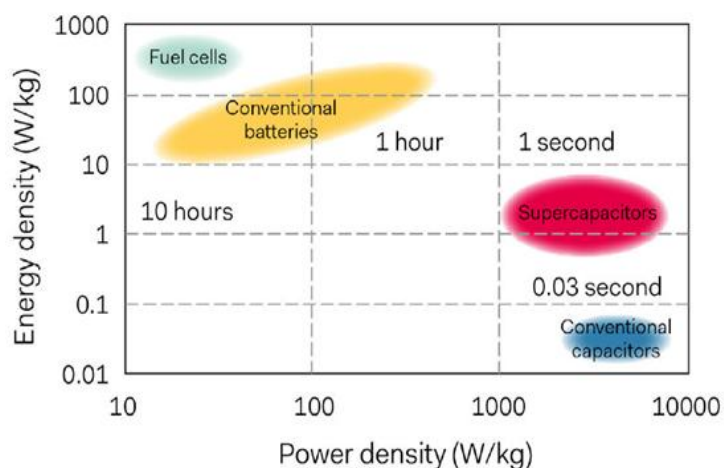
Figure 1.13 Performance comparison of supercapacitors and batteries on Ragone plot [111].

Traditionally, batteries have accomplished the role of energy storing *via* redox reactions at the electrodes during charging and discharging. However, the flammable organic solvents used in batteries can cause explosion due to short circuits. Moreover, swelling of the batteries due to dissolution of the active materials makes the battery power density limited and renders a shorter life span [112]. Also, batteries take a long time in the charging and discharging process and this time-consuming process generates heat that degrades the material. In comparison to batteries, supercapacitors possess longer cycle life with no short circuit problem and shorter charge-discharge times, and thus deliver more power very quickly. Due to this advantageous nature, supercapacitors are highly targeted for applications where high-power uptake and delivery are required, e.g., most commonly for instant power supply and rehabilitation of stop-and-go systems, industrial energy management systems, electric vehicles (most prominently used in combination with lithium-ion batteries), *etc.* An efficient outcome in terms of reducing stress in batteries in case of energy application can be expected by installing a supercapacitor run in parallel with batteries allowing sufficient energy intake within a short period and levelling those peak power requirements. Unlike batteries, supercapacitors are mainly carbon based so they can strain off the supply chain of other elements like Li, Ni or Co. Hence eco-friendliness, safety and lower cost of supercapacitor material make it more desirable than battery. It is noteworthy that a conventional supercapacitor possesses an energy density with a value of 25.87 W h kg^{-1} whereas in the current technology field, a

Chapter 1

battery energy density (Tesla battery) is 269 W h kg^{-1} [113,114]. Clearly, supercapacitors are unable to replace the battery anytime soon in terms of their energy density, but it does have a major impact on the technology we depend on today.

A conventional capacitor is made up of two conducting metal plates, a cathode, and an anode plate, separated by a dielectric insulating material. Upon application of an external voltage, the two metallic plates are oppositely charged and a potential is generated. But the charges can't pass through due to the insulating material and eventually, the energy is stored which can be released upon need. For example, when a small lamp is placed in the capacitor circuit a path now exists through the lamp to flow the electrons and reach the end which has the electron shortage, powering it. However, the powering only lasts until the build-up of electrons equalizes on both sides. The potential of a capacitor to store charge (q) is characterized by capacitance (C) which can be derived from the following mathematical formulation

$$C = q/V = \varepsilon_0\varepsilon_r A/d$$

where V, ε_0, ε_r, A, and d represent the voltage across the capacitor, permittivity of free space, relative permittivity of the dielectric medium, area of the electrode, and the distance between the electrodes respectively. Energy density and power density are two inherent parameters to measure the efficiency of a capacitor. The energy stored in the capacitor (E) is the total work done in the build-up of an electric field from an uncharged state.

$$E = \int_0^Q V dq = \int_0^Q \frac{q}{C} dq = \frac{1}{2}\, Q^2/C = \frac{1}{2}\, CV^2$$

Here, dq is the small increment of charge from negative to positively charged plate upon small work done dE by the capacitor and Q is the charge stored in the capacitor. Power density (P) can be obtained by the following relation where dt is a small change in time.

$$P = dE/dt$$

Based on working principles, capacitors can be categorized into three types:

1) Electric double-layer capacitors (EDLCs):

It contains two electrodes (cathode and anode), an electrolyte, and a separator. The separator detaches the electrodes and only allows the diffusion of ions **(Figure**

1.14). EDLCs work on the same basic principle as that of conventional capacitors but exhibit better efficiency than a capacitor. When the capacitor is connected to an external voltage supplier the ions in the electrolyte move towards the pores of the oppositely charged electrode forming an alignment of positive and negative charges at the electrode surface which is called the electric double layer (Helmholtz layer). The double layer formation eventually increases the electrode surface area and reduces the distance between the electrodes allowing EDLCs to achieve higher energy density than that of conventional capacitors (C ∞ A/d). The most common EDLC materials are graphene [115], activated carbons [116], MWCNTs [117], carbon aerogels [118], etc. The charge storage capacity is enhanced at the electrode-electrolyte interface with an increase in the electrode surface area. Hence for better efficiency, materials with higher surface area are favoured.
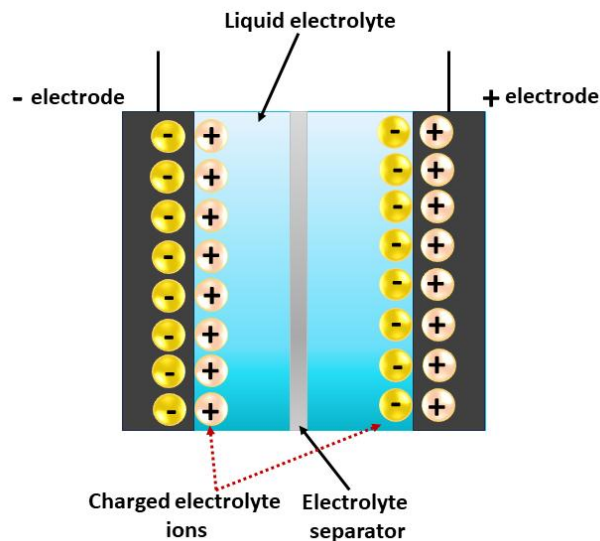
Figure 1.14 Schematic representation of the performance principle of EDLC.

2) Pseudo-capacitors

In contrast to the EDLCs. a pseudo capacitor stores charges due to the fast and reversible Faradic reactions or underpotential deposition or *via* the intercalation process. In this aspect, pseudo-capacitors are more like batteries that allow them to achieve better efficiency than EDLCs. However, due to the redox reactions, they suffer a lack of stability during cycling resulting in low power density. Its fabrication is similar to that of EDLCs but the electrodes are mainly made from metal oxides like MnO_2 [119] or from conducting polymers like polyaniline (PANI) [120], polypyrrole (PPY) [121], etc. Although it is more efficient than EDLC in terms of

energy density, most of the effective metal oxides are highly expensive and require aqueous electrolytes meaning lower voltage. Also, the electrodes are not porous like EDLCs which indicates the low surface area of the electrodes.

3) Hybrid supercapacitor

In an effort to draw the maximum energy density and capacitance, a new type of supercapacitor is generated which employs both Faradic and non-Faradic processes for charge storage. This tends to overshadow the limitations faced in EDLCs and pseudo-capacitors. The two electrodes in hybrid supercapacitors are made up of different materials. On the basis of electrode configuration, hybrid supercapacitors are of three types: composite, asymmetric and battery-type [122,123]. In a composite electrode, a carbon-based material is blended with a material used in a pseudo-capacitor in a single electrode [124] while in an asymmetric capacitor, the anode is made up of pseudo-capacitive material and the cathode is made up of EDLC material [125]. Since both the electrodes work in two different potential ranges individually, the overall device could sustain at increased potential voltage and thus a two-fold increase in energy density is obtained. The battery-type hybrid setup integrates a battery electrode with a hybrid electrode, thereby utilizing the properties of both the supercapacitor and battery [126].

1.4.1 Electrolyte materials for supercapacitor

Components of the electrolytes, both the salt and the solvent, are important constituents for supercapacitors because of their advantages in ionic conductivity and charge compensation on both the electrodes of the cell [127]. Different types of electrolytes are:

1) organic electrolytes like tetraethyl ammonium tetrafluoroborate ($TEABF_4$) dissolved in acetonitrile [128],

2) aqueous electrolytes like H_2SO_4, [129] KOH [130] and Na_2SO_4 [131],

3) ionic liquids like pyrrolidinium [132], imidazolium [133] etc., and

4) solid state polymer electrolytes like dry polymer electrolyte [134], gel polymer electrolyte [135] and polyelectrolyte [136].

1.5 Objectives

In the research area of electrocatalytic HER, there remains numerous challenges that need to be addressed. From theoretical point of view, generation of H_2 from electrocatalytic water splitting has the full potential for replacing fossil fuels but for its viable widespread implication, the process must be cost-effective, efficient, durable and accessible. So far, no catalyst has been able to satisfy all these criteria simultaneously. So, developing an electrocatalyst to address all these is still in question. As we have mentioned earlier, the most active HER electrocatalyst in an acidic medium is Pt. However, Pt is a scarce metal making the entire process quite irrelevant for practical use. An intensive study has been ongoing around the world to replace Pt with cost-effective materials. Carbon is a unique element posing numerous benefits like conductivity and corrosion resistivity along with its ability to bind with other elements, and overall increase the intrinsic property of the composite.

In our present investigation, we have tried to synthesize different nanocomposites and try to get optimum catalytic efficiency towards HER by the doping effect. Also, it is quite important to understand the role of carbon materials apart from being the structural scaffold for the metal catalysts. For the first time in 2014, Asefa and Bao reported that carbon surface can be modulated by the doping effect so that it can carry out HER efficiently [137,138]. Motivated by this study, we try to modulate the charge density around carbon by incorporating metal clusters and non-metal doping. In this thesis work, the prime focus has been on the study of the electrocatalytic activity of our synthesized nanocomposites towards HER and trying to gain insights by examining their catalytic efficiency.

The objectives of this doctoral thesis are:

i. Synthesis of different carbon-based nanocomposites:

a) Cu-doped Co_2P/ expanded graphite (EG) composite, b) Fe-doped TiO_2/ PANI nanocomposite, c) Fe-doped TiO_2/ MWCNT composite, and d) N, P-doped porous graphitic carbon.

ii. Characterisation of the as-synthesized materials by using different analytical tools.

iii. Application of the prepared materials primarily as HER electrocatalysts.

iv. Application of N, P doped carbon material as supercapacitors also.

1.6 Plan of Research

To accomplish these objectives, the following procedures will be applied.

1.6.1 Synthesis of carbon-based nanomaterials

The following synthesis procedures will be pursued

a) Traditional solvothermal process in the presence of EG to obtain Cu-doped Co_2P/EG nanocomposite.

b) An *in-situ* sol-gel technique to prepare Fe-doped TiO_2/MWCNT.

c) *In situ* chemical oxidative polymerization of PANI in present of Fe-doped TiO_2 to attain Fe-doped TiO_2/PANI composite.

d) Hierarchically porous N, P doped graphitic carbon will be synthesized using simple freeze-drying and pyrolyzed techniques.

1.6.2 Characterization of nanomaterials

Synthesized nanomaterials will be characterized by using different analytical tools like Fourier transform infrared (FTIR) spectroscopy, X-ray diffraction (XRD) technique, scanning electron microscopy (SEM), field emission scanning electron microscopy (FESEM), transmission electron microscopy (TEM), elemental dispersive X-ray (EDX) spectrometry, X-ray photoelectron spectroscopy (XPS), etc.

1.6.3 Electrochemical tests

The electrodes of the synthesized nanomaterials will be fabricated by using the drop-casting method and the catalytic properties of the materials will be investigated using linear sweep voltammetry (LSV), cyclic voltammetry (CV), electrochemical impedance spectroscopy (EIS) and chronoamperometry technique. Galvanostatic charge-discharge (GCD) analysis will be exclusively used to study the supercapacitance property of the synthesized material.

1.6.4 Application of the synthesized nanomaterials

a) Activity of the prepared catalyst will be checked towards HER with their probable reaction mechanisms discussed in chapters 2, 3, and 4.

b) Synthesized N, P-doped carbon nanomaterial will be applied both in hydrogen evolution reaction and as a symmetric supercapacitor which is discussed in Chapter 5.

1.7 References

[1] Global energy trends: Insights from the 2023 statistical review of world energy. Retrieved on 5 Aug. 2023 from https://www.forbes.com/sites/rrapier/2023/08/06/global-energy-trends-insights-from-the-2023-statistical-review-of-world-energy/?sh=156e5de43502, August 2023.

[2] CO_2 emissions in 2022. Retrieved on 5 Aug. 2023 from https://www.iea.org/reports/co2-emissions-in-2022, August 2023.

[3] Chen, X., Shen, S., Guo, L., and Mao, S.S. Semiconductor-based photocatalytic hydrogen generation. *Chemical reviews*, *110*(11):6503-6570, 2010.

[4] Ingram, D.B. (2011). *Composite Silver/Titania Photocatalysts for Visible Light Water Splitting: The Role of Silver Surface Plasmons*. PhD thesis, Department of Chemical Engineering, The University of Michigan, United States.

[5] Kleijn, R. and Van der Voet, E. Resource constraints in a hydrogen economy based on renewable energy sources: An exploration. *Renewable and Sustainable Energy Reviews*, *14*(9):2784-2795, 2010.

[6] Wang, G., Li, Y., Xu, L., Jin, Z., and Wang, Y. Facile synthesis of difunctional NiV LDH@ ZIF-67 pn junction: Serve as prominent photocatalyst for hydrogen evolution and supercapacitor electrode as well. *Renewable Energy*, *162*:535-549, 2020.

[7] Singla, M.K., Nijhawan, P., and Oberoi, A.S. Hydrogen fuel and fuel cell technology for cleaner future: a review. *Environmental Science and Pollution Research*, *28*:15607-15626, 2021.

[8] Chalgin, A., Chen, W., Xiang, Q., Wu, Y., Li, F., Shi, F., Song, C., Tao, P., Shang, W., and Wu, J. Manipulation of electron transfer between Pd and TiO_2 for improved electrocatalytic hydrogen evolution reaction performance. *ACS applied materials & interfaces*, *12*(24):27037-27044, 2020.

Chapter 1

[9] Pant, K.K. and Gupta, R.B. (2008). Fundamentals and use of hydrogen as a fuel. In *Hydrogen Fuel*, pages 15-44, ISBN:978-042-9147-36-4. In Taylor & Francis Group publication.

[10] Kothari, R., Buddhi, D., and Sawhney, R.L. Comparison of environmental and economic aspects of various hydrogen production methods. *Renewable and Sustainable Energy Reviews*, *12*(2):553-563, 2008.

[11] Hydrogen Production: Thermochemical water splitting. Retrieved on 5 Aug. 2023 from https://www.energy.gov/eere/fuelcells/hydrogen-production-thermochemical-water-splitting#:~:text=Thermochemical%20water%20splitting%20processes%20use,and%20produces%20hydrogen%20and%20oxygen, August 2023.

[12] Eroglu, E. and Melis, A. Photobiological hydrogen production: recent advances and state of the art. *Bioresource technology*, *102*(18):8403-8413, 2011.

[13] V. Dusastre. (Ed.) (2010). Materials for sustainable energy: a collection of peer-reviewed research and review articles from Nature Publishing Group. World Scientific, 360.

[14] Kirubakaran, A., Jain, S., and Nema, R.K. A review on fuel cell technologies and power electronic interface. *Renewable and sustainable energy reviews*, *13*(9):2430-2440, 2009.

[15] Barber, J. and Tran, P.D. From natural to artificial photosynthesis. *Journal of The Royal Society Interface*, *10*(81):20120984, 2013.

[16] Abas, N., Kalair, E., Kalair, A., ul Hasan, Q., and Khan, N. Nature inspired artificial photosynthesis technologies for hydrogen production: barriers and challenges. *International Journal of Hydrogen Energy*, *45*(41):20787-20799, 2020.

[17] Vidales, A.G. and Omanovic, S. Evaluation of nickel-molybdenum-oxides as cathodes for hydrogen evolution by water electrolysis in acidic, alkaline, and neutral media. *Electrochimica Acta*, *262*:115-123, 2018.

[18] Wang, H., Li, W., Liu, T., Liu, X., and Hu, X. Thermodynamic analysis and optimization of photovoltaic/thermal hybrid hydrogen generation system based on complementary combination of photovoltaic cells and proton exchange membrane electrolyzer. *Energy conversion and management*, *183*:97-108, 2019.

[19] Yu, S.C., Huang, C.W., Liao, C.H., Wu, J.C., Chang, S.T., and Chen, K.H. A novel membrane reactor for separating hydrogen and oxygen in photocatalytic water splitting. *Journal of membrane science*, *382*(1-2):291-299, 2011.

[20] Dholam, R., Patel, N., Adami, M., and Miotello, A. Hydrogen production by photocatalytic water-splitting using Cr-or Fe-doped TiO_2 composite thin films photocatalyst. *International Journal of Hydrogen Energy*, *34*(13):5337-5346, 2009.

[21] Mehtab, A., Alshehri, S.M., and Ahmad, T. Photocatalytic and photoelectrocatalytic water splitting by porous g-C_3N_4 nanosheets for hydrogen generation. *ACS Applied Nano Materials*, *5*(9):12656-12665, 2022.

[22] Fujishima, A. and Honda, K. Electrochemical photolysis of water at a semiconductor electrode. *nature*, *238*(5358):37-38, 1972.

[23] Narayanan, H., Viswanathan, B., Krishnamurthy, K.R., and Nair, H. Hydrogen from photo-electrocatalytic water splitting. *Solar Hydrogen Production*:419-486, 2019.

[24] Nozik, A.J. and Memming, R. Physical chemistry of semiconductor− liquid interfaces. *The Journal of Physical Chemistry*, *100*(31):13061-13078, 1996.

[25] Lee, J.S. Photocatalytic water splitting under visible light with particulate semiconductor catalysts. *Catalysis surveys from Asia*, *9*:217-227, 2005.

[26] Ahmad, H., Kamarudin, S.K., Minggu, L.J., and Kassim, M. Hydrogen from photo-catalytic water splitting process: A review. *Renewable and Sustainable Energy Reviews*, *43*:599-610, 2015.

[27] Du, X., Huang, J., Zhang, J., Yan, Y., Wu, C., Hu, Y., Yan, C., Lei, T., Chen, W., Fan, C., and Xiong, J. Modulating electronic structures of inorganic nanomaterials for efficient electrocatalytic water splitting. *Angewandte Chemie International Edition*, *58*(14):4484-4502, 2019.

[28] Ringe, S. Cation effects on electrocatalytic reduction processes at the example of the hydrogen evolution reaction. *Current Opinion in Electrochemistry*:101268,2023.

[29] Li, Y., Wei, X., Chen, L., and Shi, J. Electrocatalytic hydrogen production trilogy. *Angewandte Chemie International Edition*, *60*(36):19550-19571, 2021.

[30] Anantharaj, S., Ede, S.R., Sakthikumar, K., Karthick, K., Mishra, S., and Kundu, S. Recent trends and perspectives in electrochemical water splitting with an emphasis on sulfide, selenide, and phosphide catalysts of Fe, Co, and Ni: a review. *Acs Catalysis*, *6*(12):8069-8097, 2016.

[31] Ji, X., Wang, K., Zhang, Y., Sun, H., Zhang, Y., Ma, T., Ma, Z., Hu, P., and Qiu, Y. MoC based Mott–Schottky electrocatalyst for boosting the hydrogen evolution reaction performance. *Sustainable Energy & Fuels*, *4*(1):407-416, 2020.

[32] Kibsgaard, J., Tsai, C., Chan, K., Benck, J.D., Nørskov, J.K., Abild-Pedersen, F., and Jaramillo, T.F. Designing an improved transition metal phosphide catalyst for hydrogen evolution using experimental and theoretical trends. *Energy & Environmental Science*, *8*(10):3022-3029, 2015.

[33] Zhang, H., Luo, Y., Chu, P.K., Liu, Q., Liu, X., Zhang, S., Luo, J., Wang, X., and Hu, G. Recent advances in non-noble metal-based bifunctional electrocatalysts for overall seawater splitting. *Journal of Alloys and Compounds*:166113, 2022.

[34] Salmazo, D.H.C. (2018). *Theoretical investigation of the hydrogen electrocatalysis in alkaline media on bimetallic Ni-based electrodes.* PhD thesis, Université de Strasbourg, France.

[35] Laursen, A.B., Varela, A.S., Dionigi, F., Fanchiu, H., Miller, C., Trinhammer, O.L., Rossmeisl, J., and Dahl, S. Electrochemical hydrogen evolution: Sabatier's principle and the volcano plot. *Journal of Chemical Education*, *89*(12):1595-1599, 2012.

[36] Bonde, J., Moses, P.G., Jaramillo, T.F., Nørskov, J.K., and Chorkendorff, I. Hydrogen evolution on nano-particulate transition metal sulfides. *Faraday discussions*, *140*:219-231, 2009.

[37] Di Giovanni, C., Wang, W.A., Nowak, S., Grenèche, J.M., Lecoq, H., Mouton, L., Giraud, M., and Tard, C. Bioinspired iron sulfide nanoparticles for cheap and long-lived electrocatalytic molecular hydrogen evolution in neutral water. *Acs Catalysis*, *4*(2):681-687, 2014.

[38] Vandenborre, H., Vermeiren, P., and Leysen, R. Hydrogen evolution at nickel sulphide cathodes in alkaline medium. *Electrochimica acta*, *29*(3):297-301, 1984.

[39] Feng, W., Pang, W., Xu, Y., Guo, A., Gao, X., Qiu, X., and Chen, W. Transition metal selenides for electrocatalytic hydrogen evolution reaction. *ChemElectroChem*, *7*(1):31-54, 2020.

[40] Shi, Y. and Zhang, B. Recent advances in transition metal phosphide nanomaterials: synthesis and applications in hydrogen evolution reaction. *Chemical Society Reviews*, *45*(6):1529-1541, 2016.

[41] Zhang, H., Li, Y., Zhang, G., Wan, P., Xu, T., Wu, X., and Sun, X. Highly crystallized cubic cattierite CoS_2 for electrochemically hydrogen evolution over wide pH range from 0 to 14. *Electrochimica Acta*, *148*:170-174, 2014.

[42] You, B., Jiang, N., Sheng, M., and Sun, Y. Microwave vs. solvothermal synthesis of hollow cobalt sulfide nanoprisms for electrocatalytic hydrogen evolution and supercapacitors. *Chemical Communications*, *51*(20):4252-4255, 2015.

[43] Faber, M.S., Lukowski, M.A., Ding, Q., Kaiser, N.S., and Jin, S. Earth-abundant metal pyrites (FeS$_2$, CoS$_2$, NiS$_2$, and their alloys) for highly efficient hydrogen evolution and polysulfide reduction electrocatalysis. *The Journal of Physical Chemistry C*, *118*(37):21347-21356, 2014.

[44] Pataniya, P.M., Patel, V., Sahatiya, P., Late, D.J., and Sumesh, C.K. Hydrogen evolution reaction in acidic and basic medium on robust cobalt sulphide electrocatalyst. *Surfaces and Interfaces*, *34*:102319, 2022.

[45] Shen, M., Ruan, C., Chen, Y., Jiang, C., Ai, K., and Lu, L. Covalent entrapment of cobalt–iron sulfides in N-doped mesoporous carbon: Extraordinary bifunctional electrocatalysts for oxygen reduction and evolution reactions. *ACS applied materials & interfaces*, *7*(2):1207-1218, 2015.

[46] Irshad, A. and Munichandraiah, N. Electrodeposited nickel–cobalt–sulfide catalyst for the hydrogen evolution reaction. *ACS applied materials & interfaces*, *9*(23):19746-19755, 2017.

[47] Yan, Y., Xia, B., Xu, Z., and Wang, X. Recent development of molybdenum sulfides as advanced electrocatalysts for hydrogen evolution reaction. *Acs Catalysis*, *4*(6):1693-1705, 2014.

[48] Pu, Z., Luo, Y., Asiri, A.M., and Sun, X. Efficient electrochemical water splitting catalyzed by electrodeposited nickel diselenide nanoparticles based film. *ACS applied materials & interfaces*, *8*(7):4718-4723, 2016.

[49] Tang, C., Cheng, N., Pu, Z., Xing, W., and Sun, X. NiSe nanowire film supported on nickel foam: an efficient and stable 3D bifunctional electrode for full water splitting. *Angewandte Chemie*, *127*(32):9483-9487, 2015.

[50] Kong, D., Wang, H., Lu, Z., and Cui, Y. CoSe$_2$ nanoparticles grown on carbon fiber paper: an efficient and stable electrocatalyst for hydrogen evolution reaction. *Journal of the American Chemical Society*, *136*(13):4897-4900, 2014.

[51] Ullah, K., Lei, Z., Ye, S., Ali, A., and Oh, W.C. Microwave synthesis of a CoSe$_2$/graphene–TiO$_2$ heterostructure for improved hydrogen evolution from aqueous solutions in the presence of sacrificial agents. *RSC advances*, *5*(24):18841-18849, 2015.

[52] Gao, D., Xia, B., Zhu, C., Du, Y., Xi, P., Xue, D., Ding, J., and Wang, J. Activation of the MoSe$_2$ basal plane and Se-edge by B doping for enhanced hydrogen evolution. *Journal of Materials Chemistry A*, *6*(2):510-515, 2018.

Chapter 1

[53] Huang, Z., Chen, Z., Chen, Z., Lv, C., Humphrey, M.G., and Zhang, C. Cobalt phosphide nanorods as an efficient electrocatalyst for the hydrogen evolution reaction. *Nano Energy*, *9*:373-382, 2014.

[54] Zhu, Y.P., Liu, Y.P., Ren, T.Z., and Yuan, Z.Y. Self-supported cobalt phosphide mesoporous nanorod arrays: a flexible and bifunctional electrode for highly active electrocatalytic water reduction and oxidation. *Advanced Functional Materials*, *25*(47):7337-7347, 2015.

[55] Xiong, D., Wang, X., Li, W., and Liu, L. Facile synthesis of iron phosphide nanorods for efficient and durable electrochemical oxygen evolution. *Chemical communications*, *52*(56):8711-8714, 2016.

[56] Han, A., Jin, S., Chen, H., Ji, H., Sun, Z., and Du, P. A robust hydrogen evolution catalyst based on crystalline nickel phosphide nanoflakes on three-dimensional graphene/nickel foam: high performance for electrocatalytic hydrogen production from pH 0–14. *Journal of Materials Chemistry A*, *3*(5):1941-1946, 2015.

[57] Xiao, P., Sk, M.A., Thia, L., Ge, X., Lim, R.J., Wang, J.Y., Lim, K.H., and Wang, X. Molybdenum phosphide as an efficient electrocatalyst for the hydrogen evolution reaction. *Energy & Environmental Science*, *7*(8):2624-2629, 2014.

[58] Kibsgaard, J., Tsai, C., Chan, K., Benck, J.D., Nørskov, J.K., Abild-Pedersen, F., and Jaramillo, T.F. Designing an improved transition metal phosphide catalyst for hydrogen evolution using experimental and theoretical trends. *Energy & Environmental Science*, *8*(10):3022-3029, 2015.

[59] Tang, C., Gan, L., Zhang, R., Lu, W., Jiang, X., Asiri, A.M., Sun, X., Wang, J., and Chen, L. Ternary Fe x Co1–x P nanowire array as a robust hydrogen evolution reaction electrocatalyst with Pt-like activity: experimental and theoretical insight. *Nano letters*, *16*(10):6617-6621, 2016.

[60] Pan, Y., Liu, Y., Zhao, J., Yang, K., Liang, J., Liu, D., Hu, W., Liu, D., Liu, Y., and Liu, C. Monodispersed nickel phosphide nanocrystals with different phases: synthesis, characterization and electrocatalytic properties for hydrogen evolution. *Journal of Materials Chemistry A*, *3*(4):1656-1665, 2015.

[61] Ali, A., Liu, Y., Mo, R., Chen, P., and Shen, P.K. Facile one-step in-situ encapsulation of non-noble metal Co_2P nanoparticles embedded into B, N, P tri-doped carbon nanotubes for efficient hydrogen evolution reaction. *International Journal of Hydrogen Energy*, *45*(46):24312-24321, 2020.

[62] Majhi, K.C. and Yadav, M. Transition Metal-Based Chalcogenides as Electrocatalysts for Overall Water Splitting. *ACS Engineering Au*, *3*(5):278-284, 2023.

[63] Luo, Y., Tang, L., Khan, U., Yu, Q., Cheng, H.M., Zou, X., and Liu, B. Morphology and surface chemistry engineering toward pH-universal catalysts for hydrogen evolution at high current density. *Nature communications*, *10*(1):269, 2019.

[64] Chen, Z., Duan, X., Wei, W., Wang, S., and Ni, B.J. Recent advances in transition metal-based electrocatalysts for alkaline hydrogen evolution. *Journal of Materials Chemistry A*, *7*(25):14971-15005, 2019.

[65] Subbaraman, R., Tripkovic, D., Strmcnik, D., Chang, K.C., Uchimura, M., Paulikas, A.P., Stamenkovic, V., and Markovic, N.M. Enhancing hydrogen evolution activity in water splitting by tailoring Li+-Ni (OH)$_2$-Pt interfaces. *Science*, *334*(6060):1256-1260, 2011.

[66] Gong, M., Wang, D.Y., Chen, C.C., Hwang, B.J., and Dai, H. A mini review on nickel-based electrocatalysts for alkaline hydrogen evolution reaction. *Nano Research*, *9*:28-46, 2016.

[67] Ling, T., Yan, D.Y., Wang, H., Jiao, Y., Hu, Z., Zheng, Y., Zheng, L., Mao, J., Liu, H., Du, X.W., and Jaroniec, M. Activating cobalt (II) oxide nanorods for efficient electrocatalysis by strain engineering. *Nature communications*, *8*(1):1509, 2017.

[68] Li, Y., Yu, Z.G., Wang, L., Weng, Y., Tang, C.S., Yin, X., Han, K., Wu, H., Yu, X., Wong, L.M., and Wan, D. Electronic-reconstruction-enhanced hydrogen evolution catalysis in oxide polymorphs. *Nature Communications*, *10*(1):3149, 2019.

[69] Zhong, X., Sun, Y., Chen, X., Zhuang, G., Li, X., and Wang, J.G. Mo doping induced more active sites in urchin-like W18O49 nanostructure with remarkably enhanced performance for hydrogen evolution reaction. *Advanced Functional Materials*, *26*(32):5778-5786, 2016.

[70] Li, L., Zhang, T., Yan, J., Cai, X., and Liu, S. P doped MoO$_3-$x nanosheets as efficient and stable electrocatalysts for hydrogen evolution. *Small*, *13*(25):1700441, 2017.

[71] Geng, S., Liu, Y., Yu, Y.S., Yang, W., and Li, H. Engineering defects and adjusting electronic structure on S doped MoO$_2$ nanosheets toward highly active hydrogen evolution reaction. *Nano Research*, *13*:121-126, 2020.

[72] Zhong, C., Han, Z., Wang, T., Wang, Q., Shen, Z., Zhou, Q., Wang, J., Zhang, S., Jin, X., Li, S., and Wang, P. Aliovalent fluorine doping and anodization-induced amorphization enable bifunctional catalysts for efficient water splitting. *Journal of Materials Chemistry A*, *8*(21):10831-10838, 2020.

[73] Swaminathan, J., Subbiah, R., and Singaram, V. Defect-Rich Metallic Titania (TiO$_{1.23}$)☐ An Efficient Hydrogen Evolution Catalyst for Electrochemical Water Splitting. *ACS Catalysis*, *6*(4):2222-2229, 2016.

[74] Zhu, Y.P., Ma, T.Y., Jaroniec, M., and Qiao, S.Z. Self-templating synthesis of hollow Co$_3$O$_4$ microtube arrays for highly efficient water electrolysis. *Angewandte Chemie International Edition*, *56*(5):1324-1328, 2017.

[75] Hua, B., Li, M., Pang, W., Tang, W., Zhao, S., Jin, Z., Zeng, Y., Amirkhiz, B.S., and Luo, J.L. Activating p-blocking centers in perovskite for efficient water splitting. *Chem*, *4*(12):2902-2916, 2018.

[76] Guan, D., Zhou, J., Huang, Y.C., Dong, C.L., Wang, J.Q., Zhou, W., and Shao, Z. Screening highly active perovskites for hydrogen-evolving reaction via unifying ionic electronegativity descriptor. *Nature communications*, *10*(1):3755, 2019.

[77] Zhang, J., Cui, R., Gao, C., Bian, L., Pu, Y., Zhu, X., Li, X.A., and Huang, W. Cation-modulated HER and OER activities of hierarchical VOOH hollow architectures for high-efficiency and stable overall water splitting. *Small*, *15*(47):1904688, 2019.

[78] Ding, P., An, H., Zellner, P., Guan, T., Gao, J., Müller-Buschbaum, P., Weckhuysen, B.M., van der Stam, W., and Sharp, I.D. Elucidating the roles of nafion/solvent formulations in copper-catalyzed CO$_2$ electrolysis. *ACS catalysis*, *13*(8):5336-5347, 2023.

[79] McGovern, M.S., Garnett, E.C., Rice, C., Masel, R.I., and Wieckowski, A. Effects of Nafion as a binding agent for unsupported nanoparticle catalysts. *Journal of Power Sources*, *115*(1):35-39, 2003.

[80] Mishra, I.K., Zhou, H., Sun, J., Qin, F., Dahal, K., Bao, J., Chen, S., and Ren, Z. Hierarchical CoP/Ni$_5$P$_4$/CoP microsheet arrays as a robust pH-universal electrocatalyst for efficient hydrogen generation. *Energy & Environmental Science*, *11*(8):2246-2252, 2018.

[81] Yang, C., Gao, M.Y., Zhang, Q.B., Zeng, J.R., Li, X.T., and Abbott, A.P. In-situ activation of self-supported 3D hierarchically porous Ni$_3$S$_2$ films grown on nanoporous copper as excellent pH-universal electrocatalysts for hydrogen evolution reaction. *Nano Energy*, *36*:85-94, 2017.

[82] Hui, B., Zhang, K., Xia, Y., and Zhou, C. Natural multi-channeled wood frameworks for electrocatalytic hydrogen evolution. *Electrochimica Acta*, *330*:135274, 2020.

[83] Li, Y., Zhang, H., Xu, T., Lu, Z., Wu, X., Wan, P., Sun, X., and Jiang, L. Under-water superaerophobic pine-shaped Pt nanoarray electrode for ultrahigh-performance hydrogen evolution. *Advanced Functional Materials*, *25*(11):1737-1744, 2015.

[84] Zhang, C., Luo, Y., Tan, J., Yu, Q., Yang, F., Zhang, Z., Yang, L., Cheng, H.M., and Liu, B. High-throughput production of cheap mineral-based two-dimensional electrocatalysts for high-current-density hydrogen evolution. *Nature Communications*, *11*(1):3724, 2020.

[85] Jing, S., Zhang, L., Luo, L., Lu, J., Yin, S., Shen, P.K., and Tsiakaras, P. N-doped porous molybdenum carbide nanobelts as efficient catalysts for hydrogen evolution reaction. *Applied Catalysis B: Environmental*, *224*:533-540, 2018.

[86] Zheng, Z., Yu, L., Gao, M., Chen, X., Zhou, W., Ma, C., Wu, L., Zhu, J., Meng, X., Hu, J., and Tu, Y. Boosting hydrogen evolution on MoS_2 via co-confining selenium in surface and cobalt in inner layer. *Nature communications*, *11*(1):3315, 2020.

[87] Greeley, J., Nørskov, J.K., Kibler, L.A., El-Aziz, A.M., and Kolb, D.M. Hydrogen evolution over bimetallic systems: Understanding the trends. *ChemPhysChem*, *7*(5):1032-1035, 2006.

[88] Kresse, G. and Furthmüller, J. Efficiency of ab-initio total energy calculations for metals and semiconductors using a plane-wave basis set. *Computational materials science*, *6*(1):15-50, 1996.

[89] Jiang, P., Huang, H., Diao, J., Gong, S., Chen, S., Lu, J., Wang, C., Sun, Z., Xia, G., Yang, K., and Yang, Y. Improving electrocatalytic activity of iridium for hydrogen evolution at high current densities above $1000\,\mathrm{mA\,cm^{-2}}$. *Applied Catalysis B: Environmental*, *258*:117965, 2019.

[90] Yu, Y., Huang, S.Y., Li, Y., Steinmann, S.N., Yang, W., and Cao, L. Layer-dependent electrocatalysis of MoS2 for hydrogen evolution. *Nano letters*, *14*(2):553-558, 2014.

[91] Chen, Y., Yu, G., Chen, W., Liu, Y., Li, G.D., Zhu, P., Tao, Q., Li, Q., Liu, J., Shen, X., and Li, H. Highly active, nonprecious electrocatalyst comprising borophene subunits for the hydrogen evolution reaction. *Journal of the American Chemical Society*, *139*(36):12370-12373, 2017.

[92] Jagadeesan, A.K., Thangavelu, K., and Dhananjeyan, V. (2020). *Carbon nanotubes: Synthesis, properties and applications*. BoD – Books on Demand, 294.

[93] Murthy, A.P., Madhavan, J., and Murugan, K. Recent advances in hydrogen evolution reaction catalysts on carbon/carbon-based supports in acid media. *Journal of Power Sources*, *398*:9-26, 2018.

Chapter 1

[94] Zhang, L., Jia, Y., Yan, X., and Yao, X. Activity origins in nanocarbons for the electrocatalytic hydrogen evolution reaction. *Small*, *14*(26):1800235, 2018.

[95] Zhang, K., Li, C., Zhao, Y., Yu, X., and Chen, Y. Porous one-dimensional Mo_2C– amorphous carbon composites: high-efficient and durable electrocatalysts for hydrogen generation. *Physical Chemistry Chemical Physics*, *17*(25):16609-16614, 2015.

[96] Hossain, M.D., Liu, Z., Zhuang, M., Yan, X., Xu, G.L., Gadre, C.A., Tyagi, A., Abidi, I.H., Sun, C.J., Wong, H., and Guda, A. Rational design of graphene-supported single atom catalysts for hydrogen evolution reaction. *Advanced Energy Materials*, *9*(10):1803689, 2019.

[97] Heydari-Bafrooei, E. and Askari, S. Electrocatalytic activity of MWCNT supported Pd nanoparticles and MoS_2 nanoflowers for hydrogen evolution from acidic media. *International Journal of Hydrogen Energy*, *42*(5):2961-2969, 2017.

[98] Cui, C., Cheng, R., Zhang, H., Zhang, C., Ma, Y., Shi, C., Fan, B., Wang, H., and Wang, X. Ultrastable MXene@ Pt/SWCNTs' nanocatalysts for hydrogen evolution reaction. *Advanced Functional Materials*, *30*(47):2000693, 2020.

[99] Lin, C., Gao, Z., and Jin, J. Boosting Alkaline Hydrogen Evolution Activity with Ni-Doped MoS_2/Reduced Graphene Oxide Hybrid Aerogel. *ChemSusChem*, *12*(2):457-466, 2019.

[100] Chen, J., Aliasgar, M., Zamudio, F.B., Zhang, T., Zhao, Y., Lian, X., Wen, L., Yang, H., Sun, W., Kozlov, S.M. and Chen, W., 2023. Diversity of platinum-sites at platinum/fullerene interface accelerates alkaline hydrogen evolution. *Nature Communications*, *14*(1), p.1711.

[101] Jing, S., Zhang, L., Luo, L., Lu, J., Yin, S., Shen, P.K., and Tsiakaras, P. N-doped porous molybdenum carbide nanobelts as efficient catalysts for hydrogen evolution reaction. *Applied Catalysis B: Environmental*, *224*:533-540, 2018.

[102] Jiao, L., Zhou, Y.X., and Jiang, H.L. Metal–organic framework-based CoP/reduced graphene oxide: high-performance bifunctional electrocatalyst for overall water splitting. *Chemical Science*, *7*(3):1690-1695, 2016.

[103] Bard, A.J., Faulkner, L.R., and White, H.S. (2022). *Electrochemical methods: fundamentals and applications*. John Wiley & Sons, 3rd edition.

[104] Bockris, J.M., Reddy, A.K.N., Gamboa-Aldeco, M., and Peter, L.M. Comprehensive Modern Electrochemistry: Modern Electrochemistry, in 3 Volumes: Volume 1 Ionics, 1998, 767 pages, Volume 2A Fundamentals of Electrodics, 2000, 763 pages, Volume 2B Electrodics in Chemistry, Engineering, Biology and Environmental Science, 2000, 514 pages. *Platinum Metals Review*, *46*(1):15-17, 2002.

[105] Xiao, M., Miao, Y., Tian, Y., and Yan, Y. Synthesizing nanoparticles of Co-P-Se compounds as electrocatalysts for the hydrogen evolution reaction. *Electrochimica Acta*, *165*:206-210, 2015.

[106] Oh, J., Yuan, H.C., and Branz, H.M. An 18.2%-efficient black-silicon solar cell achieved through control of carrier recombination in nanostructures. *Nature nanotechnology*, *7*(11):743-748, 2012.

[107] Kerr, M.J., Schmidt, J., Cuevas, A., and Bultman, J.H. Surface recombination velocity of phosphorus-diffused silicon solar cell emitters passivated with plasma enhanced chemical vapor deposited silicon nitride and thermal silicon oxide. *Journal of applied physics*, *89*(7):3821-3826, 2001.

[108] Zhai, W., Ma, Y., Chen, D., Ho, J.C., Dai, Z., and Qu, Y. Recent progress on the long-term stability of hydrogen evolution reaction electrocatalysts. *InfoMat*, *4*(9):12357, 2022.

[109] Ding, J., Yang, H., Zhang, S., Liu, Q., Cao, H., Luo, J., and Liu, X. Advances in the electrocatalytic hydrogen evolution reaction by metal nanoclusters-based materials. *Small*, *18*(52):2204524, 2022.

[110] Kularatna, N. and Gunawardane, K. (2021). *Energy Storage Devices for Renewable Energy-Based Systems: Rechargeable Batteries and Supercapacitors*. Academic Press, 2nd edition.

[111] Will supercapacitors supersede batteries. Retrieved on 5 Aug. 2023 from https://www.electronicsweekly.com/news/design/will-supercapacitors-supersede-batteries-2018-11/, August 2023.

[112] Hu,L. and Xu, k. Nonflammable electrolyte enhances battery safety. Proceedings of the National Academy of Sciences, 111(9):3205-3206, 2014.

[113] Sun, J., Luo, B., and Li, H. A review on the conventional capacitors, supercapacitors, and emerging hybrid Ion capacitors: Past, present, and future. *Advanced Energy and Sustainability Research*, *3*(6):2100191, 2022.

[114] What do battery energy density improvements really mean for trucks, ships, & plans? Retrieved on 9 Nov. 2023 from https://cleantechnica.com/2023/05/24/what-do-battery-energy-density-improvements-really-mean-for-trucks-ships planes/#:~:text=The%20batteries%20Tesla%20uses%20have,40%2D225%20Wh%2Fkg, Nov 2023.

[115] Yang, H., Kannappan, S., Pandian, A.S., Jang, J.H., Lee, Y.S., and Lu, W. Graphene supercapacitor with both high power and energy density. *Nanotechnology*, *28*(44):445401, 2017.

[116] Subramanian, V., Luo, C., Stephan, A.M., Nahm, K.S., Thomas, S., and Wei, B. Supercapacitors from activated carbon derived from banana fibers. *The Journal of Physical Chemistry C*, *111*(20):7527-7531, 2007.

[117] Frackowiak, E. and Beguin, F. Electrochemical storage of energy in carbon nanotubes and nanostructured carbons. *Carbon*, *40*(10):1775-1787, 2002.

[118] Qian, H., Kucernak, A.R., Greenhalgh, E.S., Bismarck, A., and Shaffer, M.S. Multifunctional structural supercapacitor composites based on carbon aerogel modified high performance carbon fiber fabric. *ACS applied materials & interfaces*, *5*(13):6113-6122, 2013.

[119] Xie, X., Zhang, C., Wu, M.B., Tao, Y., Lv, W., and Yang, Q.H. Porous MnO_2 for use in a high performance supercapacitor: replication of a 3D graphene network as a reactive template. *Chemical Communications*, *49*(94):11092-11094, 2013.

[120] Shen, K., Ran, F., Zhang, X., Liu, C., Wang, N., Niu, X., Liu, Y., Zhang, D., Kong, L., Kang, L., and Chen, S. Supercapacitor electrodes based on nano-polyaniline deposited on hollow carbon spheres derived from cross-linked co-polymers. *Synthetic Metals*, *209*:369-376, 2015.

[121] Lu, P., Ohlckers, P., and Chen, X.Y. November. On-chip supercapacitor electrode based on polypyrrole deposited into nanoporous Au scaffold. *Journal of Physics: Conference Series*, 773(1):012054, 2016.

[122] Iro, Z.S., Subramani, C., and Dash, S.S. A brief review on electrode materials for supercapacitor. *Int. J. Electrochem. Sci*, *11*(12):10628-10643, 2016.

[123] Muzaffar, A., Ahamed, M.B., Deshmukh, K., and Thirumalai, J. A review on recent advances in hybrid supercapacitors: Design, fabrication and applications. *Renewable and sustainable energy reviews*, *101*:123-145, 2019.

[124] Jurewicz, K., Delpeux, S., Bertagna, V., Beguin, F., and Frackowiak, E. Supercapacitors from nanotubes/polypyrrole composites. *Chemical Physics Letters*, *347*(1-3):36-40, 2001.

[125] Fan, Z., Yan, J., Wei, T., Zhi, L., Ning, G., Li, T., and Wei, F. Asymmetric supercapacitors based on graphene/MnO2 and activated carbon nanofiber electrodes with high power and energy density. *Advanced Functional Materials*, *21*(12):2366-2375, 2011.

[126] Li, H., Cheng, L., and Xia, Y. A hybrid electrochemical supercapacitor based on a 5 V Li-ion battery cathode and active carbon. *Electrochemical and Solid-State Letters*, *8*(9):A433, 2005.

[127] Zhong, C., Deng, Y., Hu, W., Qiao, J., Zhang, L., and Zhang, J. A review of electrolyte materials and compositions for electrochemical supercapacitors. *Chemical Society Reviews*, *44*(21):7484-7539, 2015.

[128] Chmiola, J., Yushin, G., Gogotsi, Y., Portet, C., Simon, P., and Taberna, P. L. Anomalous increase in carbon capacitance at pore sizes less than 1 nanometer. *science*, *313*(5794):1760-1763, 2006.

[129] Kierzek, K., Frackowiak, E., Lota, G., Gryglewicz, G., and Machnikowski, J. Electrochemical capacitors based on highly porous carbons prepared by KOH activation. *Electrochimica Acta*, *49*(4):515-523, 2004.

[130] Du, X., Wang, C., Chen, M., Jiao, Y., and Wang, J. Electrochemical performances of nanoparticle Fe_3O_4/activated carbon supercapacitor using KOH electrolyte solution. *The Journal of Physical Chemistry C*, *113*(6):2643-2646, 2009.

[131] Athouël, L., Moser, F., Dugas, R., Crosnier, O., Bélanger, D., and Brousse, T. Variation of the MnO_2 birnessite structure upon charge/discharge in an electrochemical supercapacitor electrode in aqueous Na_2SO_4 electrolyte. *The Journal of Physical Chemistry C*, *112*(18):7270-7277, 2008.

[132] Lazzari, M., Soavi, F., and Mastragostino, M. High voltage, asymmetric EDLCs based on xerogel carbon and hydrophobic IL electrolytes. *Journal of Power Sources*, *178*(1):490-496, 2008.

[133] Ortega, P.F., dos Santos Junior, G.A., Montoro, L.A., Silva, G.G., Blanco, C., Santamaría, R., and Lavall, R.L. $LiFePO_4$/mesoporous carbon hybrid supercapacitor based on LiTFSI/imidazolium ionic liquid electrolyte. *The Journal of Physical Chemistry C*, *122*(3):1456-1465, 2018.

[134] Zhang, X., Wang, L., Peng, J., Cao, P., Cai, X., Li, J., and Zhai, M. A flexible ionic liquid gelled $PVA-Li_2SO_4$ polymer electrolyte for semi-solid-state supercapacitors. *Advanced Materials Interfaces*, *2*(15):1500267, 2015.

[135] Yu, H., Wu, J., Fan, L., Lin, Y., Xu, K., Tang, Z., Cheng, C., Tang, S., Lin, J., Huang, M., and Lan, Z. A novel redox-mediated gel polymer electrolyte for high-performance supercapacitor. *Journal of Power Sources*, *198*:402-407, 2012.

Chapter 1

[136] Huang, Y., Zhong, M., Huang, Y., Zhu, M., Pei, Z., Wang, Z., Xue, Q., Xie, X., and Zhi, C. A self-healable and highly stretchable supercapacitor based on a dual crosslinked polyelectrolyte. *Nature communications*, *6*(1):10310, 2015.

[137] Zou, X., Huang, X., Goswami, A., Silva, R., Sathe, B.R., Mikmeková, E., and Asefa, T. Cobalt-embedded nitrogen-rich carbon nanotubes efficiently catalyze hydrogen evolution reaction at all pH values. *Angewandte Chemie*, *126*(17):4461-4465, 2014.

[138] Deng, J., Ren, P., Deng, D., Yu, L., Yang, F., and Bao, X. Highly active and durable non-precious-metal catalysts encapsulated in carbon nanotubes for hydrogen evolution reaction. *Energy & Environmental Science*, *7*(6):1919-1923, 2014.